HAL
open science

Solvent-free synthesis of a formaldehyde-free benzoxazine monomer: study of its curing acceleration effect for commercial benzoxazine

Romain Tavernier, Lérys Granado, Monique Tillard, Louis van Renterghem, Thomas-Xavier Métro, Frédéric Lamaty, Leïla Bonnaud, Jean-Marie Raquez, Ghislain David, Sylvain Caillol

To cite this version:

Romain Tavernier, Lérys Granado, Monique Tillard, Louis van Renterghem, Thomas-Xavier Métro, et al.. Solvent-free synthesis of a formaldehyde-free benzoxazine monomer: study of its curing acceleration effect for commercial benzoxazine. Polymer Chemistry, 2022, 13 (40), pp.5745-5756. 10.1039/d2py00462c . hal-03819630

HAL Id: hal-03819630

https://hal.science/hal-03819630v1

Submitted on 18 Oct 2022

HAL is a multi-disciplinary open access archive for the deposit and dissemination of scientific research documents, whether they are published or not. The documents may come from teaching and research institutions in France or abroad, or from public or private research centers.

L'archive ouverte pluridisciplinaire **HAL**, est destinée au dépôt et à la diffusion de documents scientifiques de niveau recherche, publiés ou non, émanant des établissements d'enseignement et de recherche français ou étrangers, des laboratoires publics ou privés.

Solvent-free synthesis of a formaldehyde-free benzoxazine monomer: Study of its curing acceleration effect for commercial benzoxazine

Romain Tavernier[1,2,*], Lérys Granado[1], Monique Tillard[1], Louis Van Renterghem[2], Thomas-Xavier Métro[3], Frédéric Lamaty[3], Leila Bonnaud[2], Jean-Marie Raquez[2,*], Ghislain David[1], Sylvain Caillol[1]

1. ICGM, Univ Montpellier, CNRS, ENSCM, Montpellier, France. E-Mail: romain.tavernier@gmail.com
2. Laboratory of Polymeric and Composite Materials (LPCM), Center of Innovation and Research in Materials, Materia Nova Research Center & University of Mons (UMONS), Place du Parc 20, 7000 Mons, Belgium. E-mail: jean-marie.raquez@umons.ac.be
3. IBMM, Univ Montpellier, CNRS, ENSCM, Montpellier, France.

Abstract

Polybenzoxazines are very interesting phenolic resins that are obtained from ring-opening polymerisation (ROP) of benzoxazine monomers. However, commercially available resins such as bisphenol A-aniline benzoxazine (BA-a) have found limited industrial applications, partly imparted to its high ROP temperature. To tackle this limitation, we designed a 2-substituted benzoxazine monomer bearing a phenol, Ph-fa[2]PhOH, that was obtained by different methods of solvent-free and environmentally friendly synthesis, such as ball-milling and bladeless planetary mixing. The phenol functionalisation leads to a high reactivity, thanks to an hydrogen-bond activation of the oxazine ring. Ph-fa[2]PhOH displayed one of the lowest ROP temperature ever reported (ca. 160 °C) and a low activation energy (E_α) of 40-70 kJ.mol^{-1} as determined by Vyazovkin kinetic method. The high reactivity of this monomer was advantageously exploited for the reduction of ROP temperature of the commercial BA-a benzoxazine. By studying the curing process by non-isothermal DSC after different polymerisation stages, a formulation containing 10 wt% of our new monomer with BA-a precursors,

we were able to evaluate its acceleration effect. In addition, we showed that Ph-fa[2]PhOH was able to improve the T_α of the crosslinked network by 10 °C, and the char yield by 10 %, leading to a significant improvement of the properties of commercial BA-a resin.

Introduction

Polybenzoxazine is a recent class of phenolic thermoset, based on the ring-opening polymerisation (ROP) of 1,3-benzoxazines structures. Usually synthesized from a phenol, a primary amine and formaldehyde, they have been foreseen to be used in a wide range of applications such as high-performance composites,[1] space radiation shields,[2] porous polymers for CO_2 capture,[3] heavy-metal extraction from water[4] or even shape-memory or self-healing polymers.[5]

Environmental impact has become an important concern for chemists, as it is reflected by the "ten chemical innovations that will change our world" selected by IUPAC, most of them driven by sustainability.[6] A lot of efforts have been made in order to synthesize benzoxazine monomers from renewable resources,[7] using mild or more sustainable conditions. For instance, biobased polybenzoxazines were obtained from phenols such as eugenol,[8] cardanol,[9] vanillin,[10] or biobased amines such as furfurylamine,[11] stearylamine,[12] many of those examples were summed up by Salum *et al.* in their research article[12] and recently reviewed.[13] In addition, more energy-efficient and low-waste monomer synthesis methods have shown their efficiency in order to get new benzoxazine monomers, such as solvent-free microwave heating,[14] ultrasound irradiation[15] or ball-milling.[16]

Most of the synthetic pathways leading to polymerisable 1,3-benzoxazines use formaldehyde or paraformaldehyde as a reagent. Yet formaldehyde is classified as a carcinogenic compound and its substitution is being investigated in order to reduce health hazards, especially by limiting the formaldehyde emission in the indoor environment.[17] Recently , Ohashi *et al.* were the first to report the polymerisation of 2-substituted benzoxazines,[18] where benzaldehyde was used in place of formaldehyde. Later, Pereira *et al.* demonstrated that aliphatic aldehydes such as valeraldehyde was also suitable to obtain 2-substituted benzoxazines.[19] They also showed that ortho formylation of a

phenol, *e.g.* cardanol, was an efficient route to obtain phenolic compounds suitable for 2-substituted benzoxazine synthesis. In our previous articles, we showed that the use of aromatic dialdehydes was also an interesting pathway to obtain high performance polybenzoxazine, with high char yields.[20,21] Other differently substituted 1,3-benzoxazines are also able to polymerise, and can be obtained without the use of formaldehyde, as shown recently by several groups.[22,23]

However, if these new benzoxazine monomers have shown very similar properties as formaldehyde-based ones, they also suffer from the same processing limitations as polybenzoxazine chemistry. The monomers have high melting points and their polymerisation requires high temperatures (>200 °C). The addition of curing accelerators or catalysts has been investigated for oxazine-ring unsubstituted monomers (*i.e.* 1,3-benzoxazine), such as m-phenylenediamine-formaldehyde oligomers,[24] salts such as cerium salts,[25] LiBr, NaI,[26] organocatalysts such as methyl p-toluenesulfonate[27], p-toluenesulfonic acid, 2-ethyl-4-methylimidazole,[26] or amines,[28,29] metal-organic frameworks,[30] *etc*. It has also been demonstrated that the catalyst type has an effect on the polymer structure.[31] Of note, the acceleration of benzoxazine polymerisation has been reviewed recently.[32]

Benzoxazine monomer chemical design is also of great importance. For instance, the number of oxazine rings,[33,34] the influence of their relative positions[20,35] or the formation of benzoxazine oligomers has an effect on polymerization behaviour.[36] Substituents attached to any of the constitutive moieties of benzoxazine also have an influence on the polymerisation temperature. Several articles emphasize this effect, especially the role of electron-withdrawing para substituents on the phenol, that lower the polymerisation temperatures.[37–39] Other chemical moieties have an influence on the ring-opening polymerisation. For instance, it has been shown that the presence of a carboxylic group has a catalytic effect on the ring-opening of benzoxazine, and that such monomers have low polymerisation temperatures.[40–44] The use of this type of monomer in formulations along with benzoxazines with a high polymerisation temperature is beneficial for the reduction of polymerisation temperatures. The concept of using a comonomer that has a catalytic effect is desirable, since the comonomer is included

in the network and, to a certain extent, does not have detrimental influence on the structure and properties of the thermosets. Actually, carboxylic acid-containing benzoxazine networks tend to have lower thermal stability and lower char yields due to early decarboxylation.[44] It shall be noted also that lower ROP temperature can also be observed for monomers containing phenolic methylenol moieties, and other hydroxyl moieties.[45,46]

Among the functional moieties that provide low polymerisation temperature, the presence of free phenol moieties on benzoxazine monomers have also shown some interest. First, it has been demonstrated that phenols do have an effect on the ROP of benzoxazine, by simply mixing phenols and benzoxazine monomers.[43,47–51] Consequently, several research groups designed benzoxazine monomers bearing a phenolic hydroxyl group and observed that such functional group generates low polymerisation temperatures. For instance, Lin *et al.* synthesized 4-DOPO-1,3-benzoxazine diastereomers that were bearing a phenolic moiety, that presented high melting points around 238 °C, and that showed an exotherm after the melting endotherms.[52] This behaviour reflects the high reactivity of such monomer, since it actually does not display a stable liquid state. In another paper, Lin *et al.* synthesized a monomer bearing two phenolic hydroxyl groups, with a melting temperature of 143 °C and an onset of polymerisation at approx. 165 °C.[53] The direct polymerisation after melting has been observed for nearly all the phenol-containing benzoxazine monomers.[54–59] Among those very reactive benzoxazine monomers, some present the lowest polymerisation temperatures of all benzoxazine structures. They are thus very desirable, especially since they can be used as comonomers with high temperature polymerising benzoxazines, in order to lower the whole ROP process.[56,60]

Following our commitment to the preparation of formaldehyde-free benzoxazine, we herein extend the concept of highly reactive phenol-containing benzoxazine to 2-substituted structures. In order to meet sustainable chemistry criteria, we report herein new synthetic methods to obtain 2-substituted 1,3-benzoxazines by vibrating ball-milling or by planetary mixing, without using problematic solvents regularly used for such syntheses, such as toluene, dioxane or chloroform. We thus synthesized a

formaldehyde-free benzoxazine monomer containing a phenol group, and its structure was characterized by NMR spectroscopy, FTIR and XRD. Then, the polymerisation behaviour of this benzoxazine was assessed by non-isothermal DSC, and activation energies were determined using Vyazovkin method. Commercially available benzoxazine based on bisphenol A and aniline (BA-a) has found limited applications partly because of its high polymerisation temperature (>200 °C). By taking advantage of its high reactivity, our new monomer has been studied as a potential curing accelerator for the BA-a benzoxazine. The influence of this comonomer on the thermal stability and thermo-mechanical properties of the resulting materials has been assessed.

Experimental

Materials

Para-hydroxybenzaldehyde was purchased from Sigma-Aldrich. Cyclohexane, Acetone, Methanol, Toluene and Ethyl Acetate were purchased from VWR. Deuterated solvent was purchased from Eurisotop. Furfurylaminomethylphenol was synthesized according to our previous work.[20] Commercial BA-a benzoxazine was obtained from Huntsmann under the trade name Araldite MT 3600.

Ball-milling was performed using a Retsch MM400 vibrating ball-mill, using 15 mL stainless steel jars, with three 7 mm stainless steel balls, operating at 25 Hz.

Planetary mixing was performed using a Hauschild SpeedMixer DAC 400.2 VAC-P, in 60 mL polypropylene disposable cups. Cycles of 10 min were used at the maximum speed of 2500 rpm at atmospheric pressure.

Characterization

Nuclear Magnetic Resonance (NMR) spectroscopy was performed using a 400 MHz Bruker Advance NMR spectrometer. Calibration of chemical shift was performed using residual non-deuterated solvent traces. Conversion (C) was calculated by eq. (1), considering the approximation that only the desired

product is formed during the reaction. Integration values of the aldehyde (Ha) and of the aza-acetal proton (N-CHAr-O) were respectively noted I (H_a) and I (H_b).

$$C = 1 - \frac{I\ (H_a)}{I\ (H_a) + I\ (H_b)} \tag{1}$$

Fourier Transform Infrared (FT-IR) spectroscopy was performed on a Bruker Tensor 27 in ATR configuration, equipped with a RT-DLaTGS detector and KBr beam splitter. A resolution of 4 cm^{-1} was chosen, and each sample analysis was performed using 32 scans, from 4000 to 600 cm^{-1}.

Single-crystal X-ray diffraction experiment was performed using a Bruker D8 Venture diffractometer (Incoatec IμS 3.0 Mo micro-source, MoK_α radiation, Photon II CPAD detector), at a temperature of −100 °C. The compound was recovered as regularly shaped pale-orange crystals. A small platelet (0.22 × 0.21 × 0.11 mm) was selected using a stereomicroscope equipped with a polarizing filter and checked for singularity before X-ray diffracted intensities were measured. The Apex software suite[61] was used for data collection and processing, and the SHELX programs for structure solution and refinement.[62,63] Statistical tests on the diffracted intensities clearly indicate centrosymmetry for the structure found in the monoclinic P21/n centrosymmetric space group. Reflections up to θ = 39.8° were considered to determine the unit cell parameters and the multi-scan method (SADABS) was applied to correct absorption effects. A set of 3793 unique reflections is used in the final full-matrix least-squares refinement on F^2, with anisotropic displacement parameters for all non-H atoms. Except for the phenolic H-atom, detected in the final Fourier difference and freely refined, generated H-atoms are refined using a riding model with isotropic displacement parameters equal to 1.2 times the Ueq of the parent atom.

Differential Scanning Calorimetry (DSC) : For the study of single crystals and the curing kinetics of the monomer, DSC was performed using a Netzsch F200 Maia DSC using high pressure stainless steel crucibles, sealed with gold seals. The calibration was performed using several standards (indium,

biphenyl, CsCl, bismuth). All measurements have been performed under a 70 mL·min^{-1} nitrogen flow. Unless specified for curing kinetics, DSC was performed at 10 °C·min^{-1}, from ambient temperature to 350 °C. For the determination of polymerisation exotherms, integration was performed using the Proteus software from Netzsch, using a straight baseline starting from the right part of the curve. Thus, the approximation was made that the exothermic peak started where the straight baseline crossed the DSC curve, after the melting endotherm.

For the study of BA-a, blends of BA-a with Ph-fa[2]PhOH, DSC was performed on a TA Instruments 2920 using sealed low pressure aluminium crucibles. Calibration was performed using Indium. All measurements were performed under a 88 mL·min^{-1} nitrogen flow. Measurements were performed from ambient conditions to 350 °C, at 10 °C·min^{-1}. Conversion of polymerisation reaction was calculated according to the eq (2), considering the total heat of polymerisation of pure monomers or their blends, with ΔH_i the residual enthalpy of a formulation after curing step i and ΔH_{tot} the total enthalpy of uncured formulation determined by non-isothermal DSC.

$$C = \frac{\Delta H_i}{\Delta H_{tot}} \tag{2}$$

Rheology : Rheology experiments were performed on an Anton Paar rheometer, equipped with an oven. Parallel plate disposable geometries were utilized, with a 8 mm diameter. Experiments were performed at 10 °C·min^{-1} ramp, from 50 to 300 °C, with a 1 % deformation at 1 Hz.

Thermogravimetric analysis (TGA) was performed using a TA Instruments Q50 TGA, at 10°C/min from ambient temperature to 800 °C, under a 60 mL·min^{-1} nitrogen or air flow. Monolithic samples of ca. 10 mg were analysed.

Dynamic mechanical analysis (DMA) was performed using a TA Instruments Q800 DMA, at a frequency of 1 Hz, a heating rate of 3 °C·min^{-1}, using a single cantilever clamp (17.5 mm length). Measurements

were performed under air, from ambient temperature to 280 °C. Rectangular shaped materials were used, with dimensions *l x w x t* of *ca.* 2.5 cm x 0.6 cm x 1.5 mm.

Non-isothermal curing kinetics were performed according to Vyazovkin method,[64] and following the ICTAC Kinetics Committee's recommendations.[65] All the detailed methods were published elsewhere.[66] Data were generated using 5 different heating rates, namely 5, 7.5, 10, 12.5 and 15 $K \cdot min^{-1}$.

Synthesis

The synthesis of the benzoxazine monomer 4-(3-(furan-2-ylmethyl)-3,4-dihydro-2H-benzo[e][1,3]oxazin-2-yl)phenol (abbreviated Ph-fa[2]PhOH) was performed according to the three-step method already reported starting from salicylaldehyde and furfurylamine. The detailed procedures of the first and second step were already reported in our previous paper.[21] Furfurylaminomethylphenol was then reacted with para-hydroxybenzaldehyde in solution or in solvent-free conditions according to the following procedures, and as depicted in Scheme 1.

In solution:

Typically, in a 50 mL round-bottom flask, 501.4 mg (2.5 mmol, 1 eq) of furfurylaminomethylphenol and 300.5 mg (2.5 mmol, 1 eq) of p-hydroxybenzaldehyde are introduced. Then, 20 mL of methanol are added. The clear solution is then refluxed, and reaction is followed by NMR spectroscopy until no evolution is observed. Reaction was followed for 24 hours and product was not isolated.

By ball-milling:

In stainless steel ball-mill reactors, 62.2 mg (0.31 mmol, 1 eq) of furfurylaminomethylphenol and 37.5 mg (0.31 mmol, 1 eq) of para-hydroxybenzaldehyde were introduced, with 3 stainless steel balls of 7 mm diameter. Frequency was set at 25 Hz and milling time was varied. When varying the reactant ratios, the total weight of reactants was kept equal to *ca.* 100 mg. Product was not isolated.

By planetary mixing:

In a 60 mL polypropylene container, 3.00 g (14.7 mmol, 1 eq) of Furfurylaminomethylphenol and 1.80 g (14.7 mmol, 1 eq) of para-hydroxybenzaldehyde were introduced. The speed was set to 2500 rpm, and the maximum mixing time of 10 minutes was repeated until the reaction media solidified (4 cycles). Recrystallisation was performed by solubilization of the product in a mixture of cyclohexane and ethyl acetate (80/20 v/v), heated at reflux. After returning to room temperature, the solution was stored at 6-8 °C until crystallisation occurred. Crystals were obtained in one of the experiments. After recrystallisation, the product yield was *ca.* 55%.

4-(3-(furan-2-ylmethyl)-3,4-dihydro-2H-benzo[e][1,3]oxazin-2-yl)phenol (Ph-fa[2]PhOH) : NMR ^{1}H (400 MHz, DMSO-d_6) δ (ppm) : 9.49 (br s, 1H), 7.60 (dd, 1H, ^{3}J=1.8 Hz, ^{4}J=0.9 Hz), 7.31 (d, 2H, ^{3}J=8.7 Hz), 7.15 (td, 1H, ^{3}J=7.4 Hz, ^{4}J=1.7 Hz), 6.98 (dd, 1H, ^{3}J=7.5 Hz, ^{4}J=1.4 Hz), 6.91 (dd, 1H, ^{3}J=8.2 Hz, ^{4}J=1.1 Hz), 6.84 (td, 1H, ^{3}J=11.1 Hz, ^{4}J=1.2 Hz), 6.77 (d, 2H, ^{3}J=11.1 Hz), 6.40 (dd, 1H, ^{3}J=3.2 Hz, ^{4}J=1.8 Hz), 6.29 (dd, 1H, ^{3}J=3.2 Hz, ^{4}J=0.8 Hz), 5.92 (s, 1H), 3.87 (d, 1H, ^{3}J=16.9 Hz), 3.72 (d, 1H, ^{3}J=15.5 Hz), 3.71 (s, 2H).

NMR ^{13}C (400 MHz, DMSO-d_6) δ (ppm) : 157.20, 153.15, 152.01, 142.62, 128.73, 127.77, 127.73, 127.66, 120.49, 119.41, 116.12, 115.17, 110.43, 108.47, 89.61, 46.07, 45.92.

Samples curing

Neat BA-a and blends of benzoxazines were cured in homemade rectangular shaped moulds, designed with Teflon-glass composite sheets. Degassing was performed at 80-90 °C, under vacuum, for as long as necessary (typically 20-45 mins). Then, curing procedure was performed in a Memmert UF260 Plus programmable oven. Optimized curing program was 2h at 150 °C, 2h at 180 °C, and 1h at 220 °C. Samples were placed in the oven at the degassing temperature at the beginning of the curing program.

Results and discussion

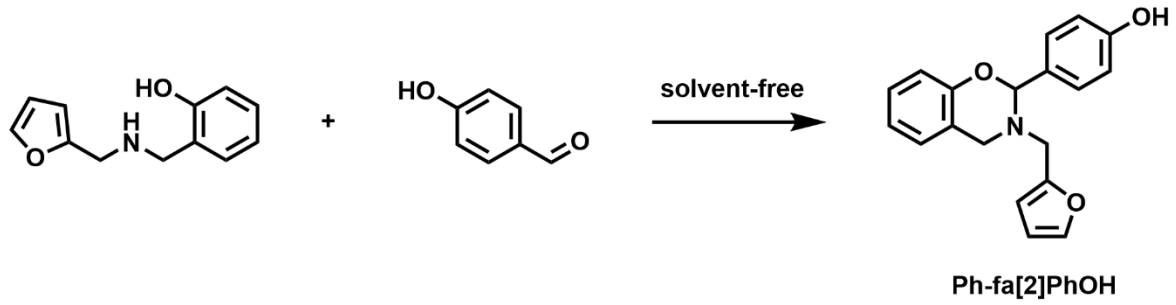

Scheme 1 - Synthetic scheme for the production of Ph-fa[2]PhOH

Ball-milling versus solution synthesis of 2-para-hydroxyphenyl benzoxazine

The formation of benzoxazine monomers usually proceeds via the condensation between amine, phenol and aldehydes, which leads to the formation of an oxazine ring. When performing the reaction with another aldehyde than formaldehyde, the main method reported for now involves the reaction between an aminomethylphenol and the aldehyde compound.[18,19,23,67–69] In order to obtain 2-substituted benzoxazines, the most reported method implies that the condensation occurs in two distinct steps. First, the primary amine is condensed with salicylaldehyde to furnish the corresponding imine. Second, the imine is reduced and then condensed with the substituted aldehyde. The use of a Dean-Stark apparatus with dehydrating solvent such as toluene can be used for this latter step. However, in our case, most probably due to the poor solubility of the aldehyde in toluene, the reaction was incomplete. The reaction was also performed in a protic and polar solvent, methanol, in view of having a better solubilisation of the reagents, including the aldehyde. Conversion attained 55 % after 3.5 h in refluxing toluene but did not improved after 7 h of reaction. Similarly, 50 % conversion was attained as a plateau after 4.7 h in refluxing methanol. Low conversion of reagents is an important drawback for the study of benzoxazine monomers, since it usually requires high purity monomers.[70] Thorough monomer purification on low conversion crudes could drastically reduce the monomer yield. We thus decided to investigate reaction conditions that would beforehand improve the reagents conversions.

The use of reaction conditions that are tolerant to heterogeneous mixtures was thought to be useful in our case. Ball-milling was used as an attempt to make the compound react in solvent-free conditions, since both homogeneous and heterogeneous mixtures with solvents failed to reach high conversions. In addition, Martina *et al.* already demonstrated that a wide range of benzoxazine design can be obtained via ball-milling.[16] In our case, ball-milling the reactants at ambient temperature for 2 hours led to conversions up to 86 %. Conversion was determined by NMR spectroscopy in deuterated DMSO-d_6. In order to ensure that the reaction did not occur during solubilisation in deuterated solvent, reagents were solubilized in DMSO-d_6 without being milled together before. Shortly after, a ^{1}H NMR spectra was acquired and showed no reaction occurred (Figure S1). All together, these results confirmed that formaldehyde-free benzoxazines can be synthesized by a solvent-free method, and that no oligomerization occurred during the milling. It is also noteworthy that the reaction proceeded at low temperature (slightly above ambient temperature due to light self-heating of the reactors during milling), contrary to other solventless procedures reported in the literature that required heating.[14,19,71,72]

Ball-milling is an advantageous synthesis process that does not require solvent or additional heat.[73] However, at the laboratory scale, less than 1 g of product could be obtained in one pot. In view of scaling up our process, we envisioned using a planetary mixer. Planetary mixers use centrifugal force to obtain homogeneous mixtures of viscous liquids or solids. Contrary to planetary ball-mills, bladeless planetary mixers do not work with beads inside reactors, and are easily scalable to the kilogram scale. Since the planetary mixer that was used in this study is not refrigerated, the duration of a mixing cycle was limited to 10 minutes, to prevent any excessive heating of the machine. NMR analysis of the crude reaction mixture was performed to monitor the conversion and to determine the optimal number of cycles to reach the highest possible conversion.

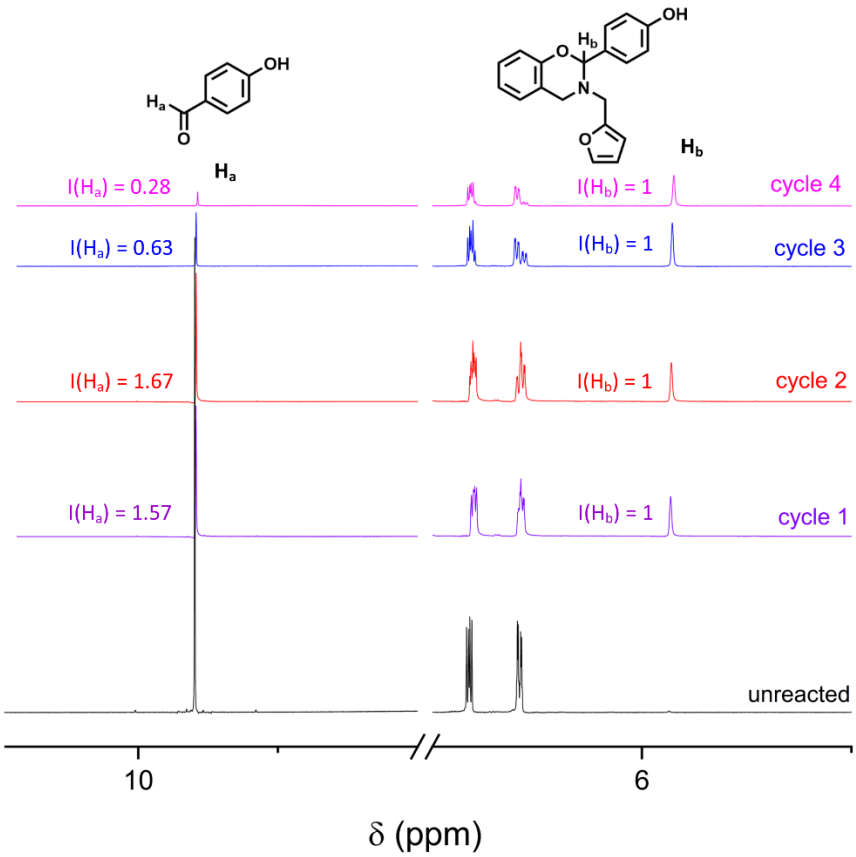

Figure 1 - ^{1}H NMR analysis of the benzoxazine formation during planetary mixing, in dmso-d_6. Each cycle represents a 10 minutes mixing step at 2500 rpm.

As it can be observed in Figure 1, after the first step of reagent mixing, a peak at ca. 5.9 ppm appears (denoted as "H_b"), corresponding to the formation of the aza-acetal moiety. While keeping the integral value of this signal constant, we can observe after each mixing step a relative decrease of the aldehyde peak of p-hydroxybenzaldehyde at ca. 9.8 ppm (denoted as "H_a"), showing the consumption of this reagent. After four cycles of 10 minutes at 2500 rpm, a stiff solid was obtained in the disposable reaction cup. Conversion attained a maximum of 78 %, corresponding to the solidification of the reaction mixture, which we assume prevented further stirring of the mixture. Yet, in order to obtain the thermal properties of the monomer, a high purity is required, since the presence of impurities influences the polymerisation characteristics.[70] Recrystallisation could be performed using a mixture of cyclohexane and ethyl acetate, and afforded single crystals of the desired product in high purity,

one of which was characterized by X-ray diffraction, as described below. After recrystallisation, Ph-fa[2]PhOH was isolated in 52 % yield.

Monomer characterizations

^{1}H and ^{13}C NMR spectroscopies have been used to characterize the new benzoxazine monomer Ph-fa[2]PhOH. On ^{1}H NMR spectra (Figure 2-a) and Figure S2), the characteristic peak of 2-substituted benzoxazine is N-CHAr-O singlet at 5.9 ppm (proton denoted “c”). Aromatic protons located on the phenol moiety attached to the oxazine ring are doublets at 7.3 and 6.8 ppm (protons denoted “k” and “f”). Methylene protons are overlapping between 3.7 and 3.9 ppm, and appear as doublets, as described before (protons denoted “a”, “b” and “b’”).[74] On ^{13}C NMR, the signal of the carbon N-CH(PhOH)-O of the oxazine appears at 89.61 ppm while the signals of the methylene carbons appear at 45.92 and 46.07 ppm. Full spectra are shown in Figure S2-3. The attribution was also supported by an APT (attached proton test) experiment, shown in Figure S4. These signals are consistent with other 2-substituted benzoxazines reported previously.[20,21,23]

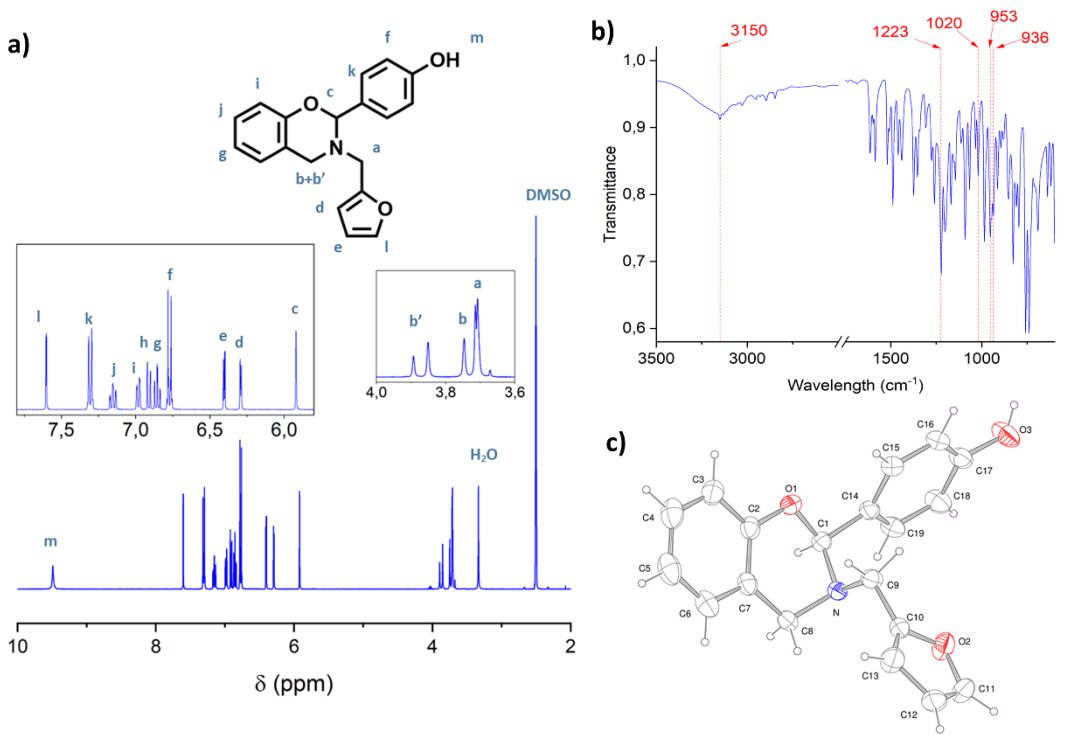

Figure 2 - Characterizations of Ph-fa[2]PhOH : a) ^{1}H NMR spectrum, b) FTIR spectrum zoomed on 2500-3500 cm^{-1} and 600-2000 cm^{-1} regions, c) Ortep representation of the $C_{19}H_{17}NO_3$ molecule (asymmetric unit) with the ellipsoids drawn at 50 % probability.

The monomer was also characterized by FT-IR spectroscopy (Figure 2-b, complete spectrum Figure S5). Characteristic bands of benzoxazine are observed, with two sharp signals at 936 and 953 cm^{-1}. Some previously reported structures displayed several bands in the same region.[20,23] We can also observe Ar-O-C bands from the heterocycle at 1020 and 1223 cm^{-1}. It is also noticeable that a broad band corresponding to free hydroxyl group is observed at 3150 cm^{-1}.

In addition, since we were able to obtain benzoxazine single crystals (see picture Figure S6), we were able to determine the full 3D structure of the monomer in its solid state. Table 1 reports the main crystal data and refinement parameters. The asymmetric unit, a molecule of formula $C_{19}H_{17}NO_3$ is represented in Figure 2-c drawn with ORTEP-3 for Windows.[75] The symmetry of space group $P\ 2_1/n$ generates four molecules in the monoclinic unit cell (a = 8.9115(6), b = 18.9555(13), c = 9.6086(8) Å, β = 104.430(3) °). As the asymmetric unit contains one asymmetric C atom (C1, displaying the S

configuration), the unit cell, therefore, contains both enantiomers of the molecule. The oxazine ring conformation can be assessed with the dihedral angle of 44.6(7) ° measured between the plane passing through C1, N, and C8 atoms and the mean plane through atoms C1, C2, C7, C8 and O1. Note the latter only deviates by 2.45(5) ° from the mean plane passing through the atoms (C2 to C7) of the benzene ring. Similarly, the furan and phenolic rings form between them a dihedral angle of 75.78(4)°, and their relative position with respect to the benzene ring is measured by dihedral angles of 32.30(5) and 46.28(4)°, respectively. Atomic coordinates, bond length, angles, and anisotropic displacement parameters are given in Tables S1-4. Complete data can be found in the CIF file, freely available with the CCDC number 2161734 at the Cambridge Crystallographic Data Centre.[76] The molecules are arranged in the crystal with their largest dimension approximately aligned along the *b* unique axis of the monoclinic cell as can be seen in Figure S7. The molecular packing is stabilized by intermolecular hydrogen bond type interactions O3−H···N (2.821Å) and, to a lesser extent, by longer interactions of 3.267Å at the C12−H···O1 atoms. These interactions give rise to a sort of layered arrangement of the molecules in diagonal planes parallel to $(10\overline{1})$, Figure 3. Literature usually reports the presence of hydrogen bonding to explain the higher reactivity of benzoxazine structures containing free phenolic moieties. However, these bonds are often assessed by NMR spectroscopy, in solution. [54,56] In our case, the interaction O3−H···N in the solid state is also in favour of an intermolecular hydrogen bond. It is also supported by the fact that polymerisation occurs directly after melting. The ability of 1,3-benzoxazines to polymerise is related to the particular conformation of the heterocycle. A certain ring tension is deduced from the different bond length and angles. Especially, around the nitrogen atom of oxazine, C1-N-C8 angle is 108.46(8) °, C1-N-C9 is 112.02(8) ° and C8-N-C9 is 110.82(8) °. Some of these sp^3 hybridization bond angles are larger than normal (109.75 °). The O1-C1 bond is longer than the phenolic O1-C2 bond (respectively 1.448(1) Å and 1.374(1) Å), and regarding N-C bonds, the intra oxazine N-C8 and N-C1 are respectively 1.480(1) and 1.462(1) Å long, comparable to N-C9 bond of 1.484(1) Å that is the 2-substitution. These length and angles correspond to similar structures reported in the literature, either furfurylamine based structures or 2-substituted structure.[77,78] These structural

characterizations further confirm that 2-substituted structures are not different than 1,3-2H benzoxazines, but might offer even more functional sites. It is also consistent with recently reported 2,4-substituted structure.[23]

Table 1 - Data collection parameters at 173 K and structure refinement details

Formula		$C_{19}H_{17}NO_3$ (Z = 4)
M, g·mol^{-1}		307.33
Calc. density, g·cm^{-3}		1.299
System, space group		Monoclinic, $P\ 2_1/n$
Unit cell, Å, °		a = 8.9115(6), b = 18.9555(13) c = 9.6086(8), β = 104.430(3)
Volume, Å^3		1571.9(2)
Collected/unique reflections		25779/3793 [R_{int} = 0.0349]
Completeness to θ = 25.242°		99.8
Data/parameter ratio		3793 / 212
Goodness-of-fit on F^2		1.036
Final indices	**[all data]**	R1 = 0.0394, wR2 = 0.1033
	[I>2σ(I)]	R1 = 0.0460, wR2 = 0.1067
Extinction coefficient		0.0051(13)
Largest peak and hole, e.Å^{-3}		0.251 and −0.202

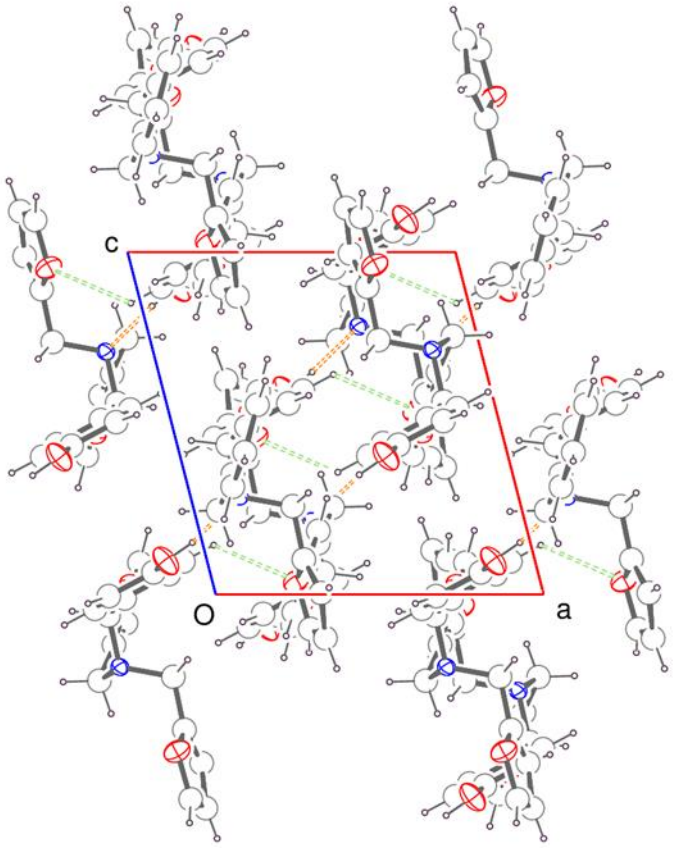

Figure 3 - The molecular packing in the crystal, viewed along the monoclinic b-unique axis The intermolecular interactions are drawn as dashed lines, green for the 3.267 Å weak O1···C12 interactions and orange for the O3···N hydrogen bonds of 2.821Å

Curing behaviour of the monomer

Non-isothermal DSC was performed on the pure monomer in order to assess the polymerisation behaviour (Figure 4-a). Using a heating rate of 10 °C·min^{-1}, a melting endotherm is observed with a maximum at 141 °C, and the polymerisation exotherm is observed just after, with no baseline between both thermal events. This very low thermal ROP is one of the lowest reported yet in the literature. The polymerisation signal appears as a bimodal peak, with two successive maxima around 160 °C and 190 °C. The enthalpy of the exotherm at 10 °C·min^{-1} is 327 J·g^{-1}, corresponding to 100 kJ·mol^{-1}. This characteristic bimodal exothermic signal is often observed for furan-containing benzoxazines, with or without substitution on the 2-position.[20,41,79] In fact, only one broad signal is generally seen.[56,80–82] Total enthalpy is also in the upper tier compared to other furan-containing structures, showing a very high reactivity of the monomer. For comparison, Zhang *et al.* obtained a naringenin and furfurylamine based monomer displaying a polymerisation with a peak temperature (T_p) of 166 °C.[56] A comparable

structure using aniline as the amine displayed a T_p of 180 °C.[54] Regarding the effect of oxazine-ring substitution, recently Mukherjee *et al.* reported enthalpies of 40 kJ·mol^{-1} for Ph-fa, 70 kJ·mol^{-1} for Ph-fa[2]Ph, compared to the pendant benzylamine with 8 kJ·mol^{-1} for Ph-ba and 13 kJ·mol^{-1} for Ph-ba[2]Ph from our previous work.[20,23] Our new monomer thus shows a very good polymerisable ability compared to previously reported substituted structures. It is also worth mentioning that the ROP behaviour of single crystals and polycrystalline form is very similar, with a shift to lower temperatures of polycrystalline monomer (of ca. 7 °C), as shown in Figure S8.

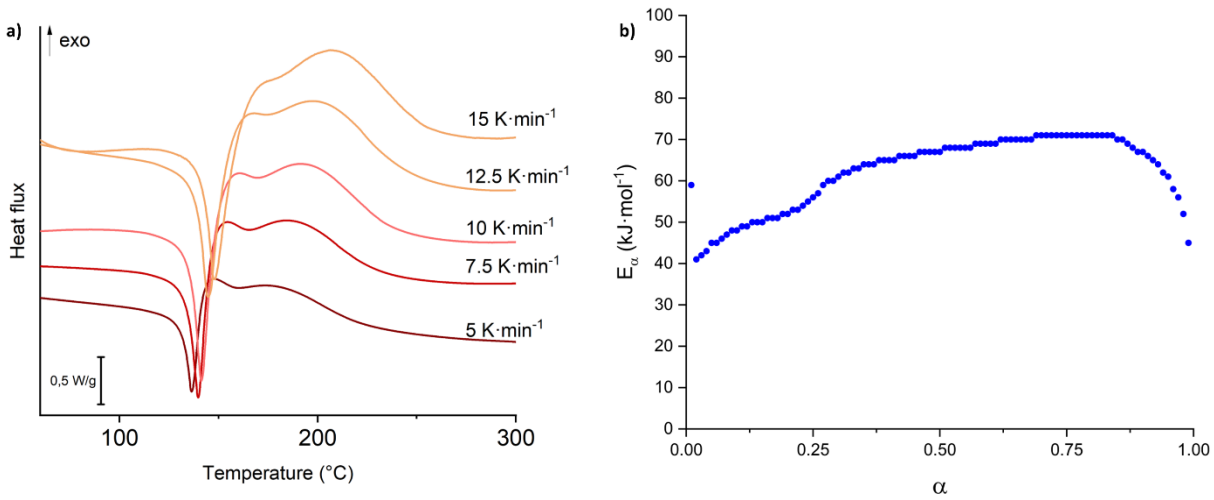

Figure 4 - a) DSC thermograms of Ph-fa[2]PhOH at different heating rates and b) Activation energy of Ph-fa[2]PhOH

In order to obtain more information on the polymerisation of the monomer, we performed non-isothermal kinetics, using Vyazovkin method.[64] The method is an integral method based on DSC thermograms at multiple heating rates (Thermograms are shown in Figure 4-a and integrals in Figure S9). The computational details can be found in our previous articles.[66,83] This method allowed us to obtain the activation energy (E_α) as a function of the conversion (α). As shown in Figure 4-b, there is nearly a continuous increase of E_α as the conversion increases. However, several regimes can be observed. First, when $\alpha < 0.25$, there is an increase in E_α from 40 to 60 kJ·mol^{-1}. Then, the E_α increases from 60 to 70 kJ·mol^{-1} for $0.25 < \alpha < 0.85$. For $\alpha > 0.85$ the E_α drops abruptly, these decreases are often attributed to increasing experimental errors near completion of the reaction. Since exothermic signals at the beginning and ending of the reaction are weak, there are more uncertainties related to the E_α

calculations. The global values of the activation energy are relatively low for a monofunctional benzoxazine, compared to what is found in the literature.[84–86] Since it is observed by XRD that phenolic hydrogen of one molecule is close to the nitrogen atom of another benzoxazine molecule, this could favour the ROP right after the melting of the monomer, leading to lower activation energies.

The two different regimes of the E_α (40-60 kJ·mol^{-1} and 60-70 kJ·mol^{-1}) are surely related to the two overlapping peaks that are observed on non-isothermal DSC thermograms (Figure 4-a). The shift between the two reactions happened for $\alpha \approx 0.25$. The increase of E_α is usually attributed to the decreased diffusion of reactive species inside the growing network.

Curing acceleration study

The curing acceleration ability of phenol-containing benzoxazine has been reported several times in literature.[53,56,57] The basic principle is to blend a given monomer with a lower curing one (an accelerator) to decrease the global polymerisation temperatures. For instance, Zhu *et al.* studied blends of pyrogallol-based benzoxazines and p-phenylenediamine-phenol (P-ddm) benzoxazine.[58] They used up to 25 wt% of pyrogallol-based accelerators. Non-isothermal DSC revealed that the onset of polymerisation was lower than in neat P-ddm but unfortunately the isothermal curing study did not allow to reach the full curing of the systems. Ren *et al.* used a pyrogallol-furfurylamine based monomer to accelerate the curing of BA-a, but they assessed the acceleration using only non-isothermal DSC.[57] If the blends showed a lower onset of polymerisation, the integral of curing exotherm clearly showed that the full conversion was attained at higher temperatures than for the neat BA-a. The same curing accelerator was used by Chen *et al.* for the acceleration of eugenol-stearylamine (E-s) benzoxazine.[87] In this paper, the authors clearly showed that the neat E-s still presented residual enthalpy after curing at 180 °C and an additional step at 220 °C was required to reach full polymerization. Nevertheless, in presence of 20 wt% of accelerator they were able to achieve full crosslinking of the system at 180 °C. If non-isothermal DSC is useful to reveal the activation of ROP at lower temperature, showing that these monomers are good ROP promoters, the acceleration should be demonstrated on a full curing

process, to our opinion. Otherwise, as it can be observed in some papers, these very reactive benzoxazines only display an acceleration effect at the beginning of the ROP, and not on the full crosslinking reaction. This effect is expected, since accelerating the initiation and propagation of the ROP will lead to an earlier vitrification of the network, requiring sometimes to increase the curing temperature, to ensure completeness of the reaction.

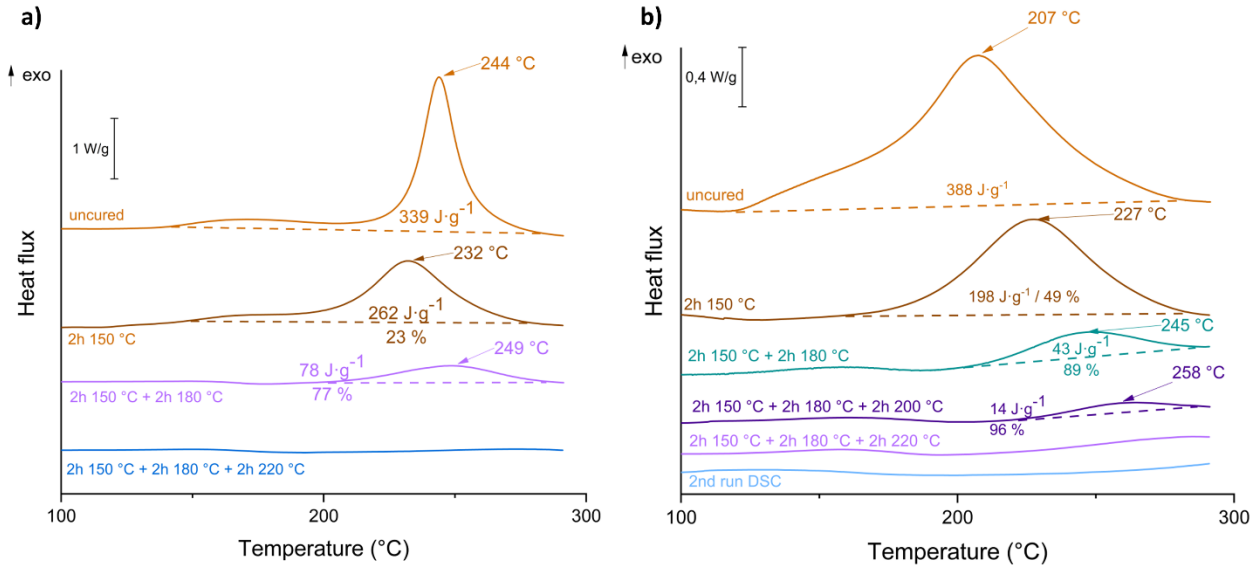

Figure 5 - Non-isothermal DSC at 10 °C·min^{-1} of a) BA-a and b) its blend with Ph-fa[2]PhOH, after different isothermal treatments

In order to assess the acceleration effect of our new monomer on the polymerisation of benzoxazines, we first observed the curing behaviour of a mixture containing 10 wt% of our monomer in commercially available BA-a benzoxazine by non-isothermal DSC at 10 °C·min^{-1}, and compared it with neat BA-a. It can be observed that the neat BA-a presents a sharp exothermic peak, with the maximum at 244 °C as expected and commonly reported in the literature (Figure 5-a). The blend with the comonomer shows a larger exothermic signal, starting from ca. 120 °C, with a peak maximum at 207 °C (Figure 5-b) highlighting the ability of the phenol-containing monomer to successfully lower the ROP temperature of BA-a.

Blends of BA-a and Ph-fa[2]PhOH were then prepared and cured following increasing isothermal steps. The conversion of reaction was assessed by non-isothermal DSC after each curing step by measuring the residual enthalpy, in order to assess the effect of the designed comonomer. It can be observed

that after 2 h at 150 °C, the neat BA-a has a very low conversion (23 %), while the blend based system reaches ca. 49 % conversion. After successive steps at 150 and 180 °C, the blend based system reaches 89 % conversion whereas the neat commercial benzoxazine only reaches 77 % conversion. Full conversion for both thermosets is achieved with an additional post-cure step of 1 hour at 220 °C.

Additional rheology experiments were also performed to confirm the acceleration for the crosslinking during the first stages of curing, as shown in Figure S10. Following the complex viscosity of both formulations at 10 °C·min^{-1} we can observe the effect of the addition of Ph-fa[2]PhOH. For both formulations, viscosity drops in the 50-100 °C range, due to the gel transition of BA-a. A transient regime is observed with a very low viscosity, under 0.1 Pa·s, and as the temperature rises, an important increase due to the ROP is observed. For the BA-a, the sharp increase of viscosity is observed around 240 °C, whereas for the formulation containing Ph-fa[2]PhOH, this increase happens 20 °C earlier.

These results show that the accelerating effect of the highly reactive monomer mainly occurs at the beginning of the polymerisation. Among the assumption that can be drawn from these results, we can postulate that a faster curing will lead to a diffusion-controlled regime earlier in the blend based system, thus slowing down the reaction at high conversion. Complete curing must then proceed at higher temperature, to overcome those limitations. In addition, the macroscopic observation of the samples reveals that the phenol-bearing monomer might not be homogeneously dispersed in the BA-a matrix (Figure S11). Thus, the optimal mixture at the molecular level might not be reached, and the acceleration effect may not be optimized. Additional pictures in Figure S12 show that whether the mixture is performed in solution (in methanol) or in melt (at degassing temperature), small clusters of Ph-fa[2]PhOH are observed. Using a mortar and pestle to homogenize the powder even leads to bigger clusters. These clusters could also reveal that taking advantage of a monomer which polymerizes right after melting could negatively lead to an early phase separation, possibly due to the poor dispersion of the Ph-fa[2]PhOH monomer. Better processes to obtain a fully homogenous mixture could improve the results.

Thermomechanical properties

Dynamic mechanical analysis has been performed on rectangular shaped samples, and are shown in Figure 6-a. These analyses have been performed under air atmosphere, from ambient temperature to 280 °C. The glassy storage modulus, at ambient temperature, was determined to be within 2.8-3.1 GPa for both pristine and blended based systems. As it was expected from the literature, the BA-a sample showed an elevated alpha-transition temperature (T_α) near 180 °C, as determined from the maximum of loss modulus. The blend based material exhibits a higher T_α, at 190 °C which is a 10 °C improvement with only 10 wt% additive while the glassy modulus remains in the same order of magnitude.

In addition, the rubbery storage modulus, as measured at T_α + 60 °C, is increased by nearly a factor two for the blended materials, reaching up 80 MPa. This quite high rubbery storage modulus suggests a highly cross-linked structure. However, at the end of the analysis, the modulus rises for this material, probably due to the beginning of degradation in air conditions at 3 °C·min^{-1} (*cf* thermal stability discussed hereafter, at 10 C·min^{-1}, under air).

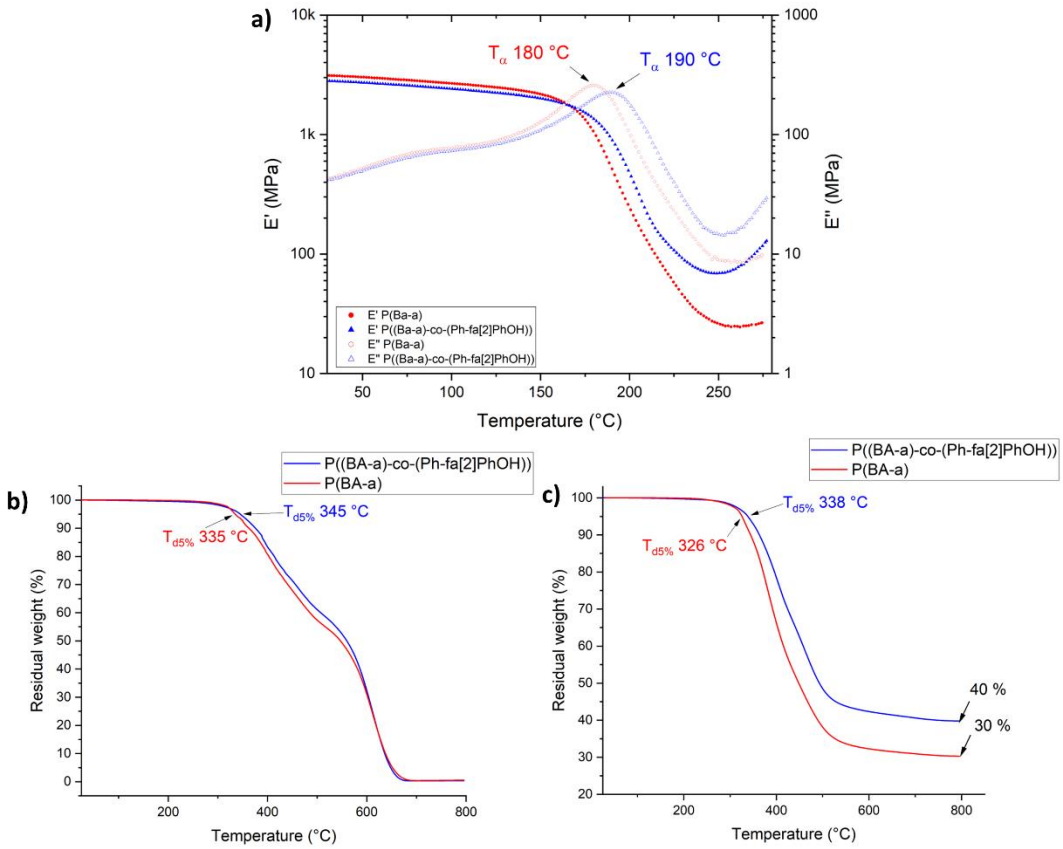

Figure 6 - Thermomechanical properties of cured samples. a) DMA under air at 1 Hz and at 3 °C·min^{-1}, b) TGA under air at 10 °C·min^{-1}, c) TGA under nitrogen at 10 °C·min^{-1}

Thermogravimetric analyses have been performed under air and under nitrogen. Under the oxidative environment, shown in Figure 6-b, both samples have similar degradation pathways, approximatively at the same temperatures. The Ph-fa[2]PhOH however shows a slightly higher $T_{d5\%}$, and it was expected since this structure has increased the aromatic content of the resin. At 800 °C, all the samples have degraded. Under an inert atmosphere, as shown in Figure 6-c, degradation of the modified BA-a happens at higher temperature, and only one weight loss is observed for both samples. At 800 °C however, char yield is 10 % higher for the modified BA-a. This is also an important improvement of the char formation, which can be explained by a higher aromatic density, but also the effect of the furan, as it is now well established.[59,88–90]

Conclusion

The substitution at the 2-position of the oxazine ring has here demonstrated its usefulness in providing another functionalization pathway for benzoxazine monomers. Ball-milling and planetary mixing have

been useful techniques to assess the feasibility of a solvent-free synthetic route, and to elaborate a scalable synthetic procedure. Monocrystals were obtained and allowed for a complete elucidation of the monomer spatial structure.

ROP kinetics were assessed by non-isothermal DSC. Again, we observed in this study a bimodal exothermic signal, suggesting a two-steps mechanism of ROP. Vyazovkin kinetic computations helped to quantify the activation energy of the two successive steps, being in the ranges of 40-60 kJ mol^{-1} and 60-70 kJ mol^{-1}, respectively. After, the study of the curing acceleration of BA-a with our newly developed and very reactive monomer has been performed. If our monomer lead to a general decrease of ROP temperature by 10 °C (maximum of exothermic DSC signal), the assessing of the acceleration by means of residual enthalpy show than the monomer generally fails to purely speed up the reaction under actual curing schedules (multi-steps isothermal). As observed generally in the literature, an important reduction of the ROP temperature of the formulation does not necessarily lead to a full acceleration of the crosslinking. It is also important to note that researchers did not always use residual enthalpy to clarify whether or not the accelerating effect can be applied to industrial processes.

Nonetheless, the monomer successfully improves the thermomechanical properties of commercial BA-a by increasing T_α by 10 °C, and also char yield by 10 %, only by adding 10 wt% additive. These results could represent a way to improve the properties of the commercial BA-a, and also give insight on how to develop a real curing accelerator for high temperature ring-opening benzoxazines.

Author Contributions

R. T. Conceptualization, Data curation, Formal analysis, Investigation, Methodology, Visualization, Writing – original draft, Writing – review & editing.

L. G. Data curation, Formal analysis, Investigation, Methodology, Software, Writing – review & editing.

M. T. Data curation, Formal analysis, Investigation, Visualization, Writing – original draft, Writing – review & editing.

L. V. R. Investigation, Writing – review & editing.

T.-X. M. Project administration, Resources, Supervision, Writing – review & editing.

F. L. Project administration, Resources, Supervision, Writing – review & editing.

L. B. Funding acquisition, Project administration, Resources, Supervision, Writing – review & editing.

J.-M. R. Funding acquisition, Project administration, Resources, Supervision, Writing – review & editing.

G. D. Project administration, Resources, Supervision, Writing – review & editing.

S. C. Project administration, Resources, Supervision, Writing – review & editing.

Conflicts of interest

There are no conflicts to declare.

Acknowledgements

R. T. thanks F. Quintin and Y. Yeboue for their help and kindness during his stay at IBMM, and also F. Cuminet for the help with data management. R. T. also thanks D. Granier and the University of Montpellier "Réseau des rayons X et gamma" for the X-ray analyses. L.B. and J-M. R. wish to thank the Wallonia-Brussels Federation, Wallonia and European Community for general support in the frame of the Concerted Research Action program (ARC 2020 - PROCOMAG project) and the INTERREG V program (ATHENS project).

References

1 B. Kiskan, N. N. Ghosh and Y. Yagci, *Polym. Int.*, 2011, **60**, 167–177.

2 D. Iguchi, S. Ohashi, G. J. E. Abarro, X. Yin, S. Winroth, C. Scott, M. Gleydura, L. Jin, N. Kanagasegar, C. Lo, C. R. Arza, P. Froimowicz and H. Ishida, *ACS Omega*, 2018, **3**, 11569–11581.
3 S. Xu, J. He, S. Jin and B. Tan, *Journal of Colloid and Interface Science*, 2018, **509**, 457–462.
4 D. Iguchi, M. L. Salum and P. Froimowicz, *Macromol. Chem. Phys.*, 2019, **220**, 1800366.
5 B. Kiskan, *Reactive and Functional Polymers*, 2018, **129**, 76–88.
6 F. Gomollón-Bel, *Chemistry International*, 2019, **41**, 12–17.
7 G. Lligadas, A. Tüzün, J. C. Ronda, M. Galià and V. Cádiz, *Polym. Chem.*, 2014, **5**, 6636–6644.
8 L. Dumas, L. Bonnaud, M. Olivier, M. Poorteman and P. Dubois, *J. Mater. Chem. A*, 2015, **3**, 6012–6018.
9 H. Arumugam, S. Krishnan, M. Chavali and A. Muthukaruppan, *New J. Chem.*, 2018, **42**, 4067–4080.
10 N. K. Sini, J. Bijwe and I. K. Varma, *Polymer Degradation and Stability*, 2014, **109**, 270–277.
11 P. Thirukumaran, A. Shakila Parveen and M. Sarojadevi, *ACS Sustainable Chem. Eng.*, 2014, **2**, 2790–2801.
12 M. L. Salum, D. Iguchi, C. R. Arza, L. Han, H. Ishida and P. Froimowicz, *ACS Sustainable Chem. Eng.*, 2018, **6**, 13096–13106.
13 Y. Lyu and H. Ishida, *Progress in Polymer Science*, 2019, **99**, 101168.
14 J. R. Oliveira, L. R. V. Kotzebue, F. W. M. Ribeiro, B. C. Mota, D. Zampieri, S. E. Mazzetto, H. Ishida and D. Lomonaco, *J. Polym. Sci. Part A: Polym. Chem.*, 2017, **55**, 3534–3544.
15 M. R. Vengatesan, S. Devaraju, D. Kannaiyan, J. K. Song and M. Alagar, *Polym. Int.*, 2013, **62**, 127–133.
16 K. Martina, L. Rotolo, A. Porcheddu, F. Delogu, S. R. Bysouth, G. Cravotto and E. Colacino, *Chem. Commun.*, 2018, **54**, 551–554.
17 T. Salthammer, S. Mentese and R. Marutzky, *Chem. Rev.*, 2010, **110**, 2536–2572.
18 S. Ohashi, F. Cassidy, S. Huang, K. Chiou and H. Ishida, *Polym. Chem.*, 2016, **7**, 7177–7184.
19 R. C. S. Pereira, L. R. V. Kotzebue, D. Zampieri, G. Mele, S. E. Mazzetto and D. Lomonaco, *Materials Today Communications*, 2019, **21**, 100629.
20 R. Tavernier, L. Granado, G. Foyer, G. David and S. Caillol, *Polymer*, 2021, **216**, 123270.
21 R. Tavernier, L. Granado, G. Foyer, G. David and S. Caillol, *Macromolecules*, 2020, **53**, 2557–2567.
22 I. Machado, I. Hsieh, E. Rachita, M. L. Salum, D. Iguchi, N. Pogharian, A. Pellot, P. Froimowicz, V. Calado and H. Ishida, *Green Chem.*, 2021, **23**, 4051–4064.
23 S. Mukherjee, N. Amarnath and B. Lochab, *Macromolecules*, 2021, **54**, 10001–10016.
24 L. Zhang, J. Mao, S. Wang, Y. Yang, Y. Chen and H. Lu, *Reactive and Functional Polymers*, 2017, **121**, 51–57.
25 T. Zhang, L. Bonnaud, J.-M. Raquez, M. Poorteman, M. Olivier and P. Dubois, *Polymers*, 2020, **12**, 415.
26 C. Liu, D. Shen, R. M. Sebastián, J. Marquet and R. Schönfeld, *Macromolecules*, 2011, **44**, 4616–4622.
27 C. Wang, C. Zhao, J. Sun, S. Huang, X. Liu and T. Endo, *J. Polym. Sci. A Polym. Chem.*, 2013, **51**, 2016–2023.
28 J. Wang, Y. Z. Xu, Y. F. Fu and X. D. Liu, *Sci Rep*, 2016, **6**, 38584.
29 A. Kocaarslan, B. Kiskan and Y. Yagci, *Polymer*, 2017, **122**, 340–346.

30 P. Sharma, M. Srivastava, B. Lochab, D. Kumar, A. Ramanan and P. K. Roy, *ChemistrySelect*, 2016, **1**, 3924–3932.
31 C. Liu, D. Shen, R. M. Sebastián, J. Marquet and R. Schönfeld, *Polymer*, 2013, **54**, 2873–2878.
32 B. Lochab, M. Monisha, N. Amarnath, P. Sharma, S. Mukherjee and H. Ishida, *Polymers*, 2021, **13**, 1260.
33 N. K. Sini and T. Endo, *Macromolecules*, 2016, **49**, 8466–8478.
34 M. Soto, M. Hiller, H. Oschkinat and K. Koschek, *Polymers*, 2016, **8**, 278.
35 S. N. Kolanadiyil, M. Minami and T. Endo, *Macromolecules*, 2017, **50**, 3476–3488.
36 K. D. Demir, B. Kiskan, B. Aydogan and Y. Yagci, *Reactive and Functional Polymers*, 2013, **73**, 346–359.
37 A. Martos, R. M. Sebastián and J. Marquet, *European Polymer Journal*, 2018, **108**, 20–27.
38 S. Ohashi, D. Iguchi, T. R. Heyl, P. Froimowicz and H. Ishida, *Polym. Chem.*, 2018, **9**, 4194–4204.
39 R. Andreu, J. A. Reina and J. C. Ronda, *J. Polym. Sci. A Polym. Chem.*, 2008, **46**, 3353–3366.
40 R. Andreu, J. A. Reina and J. C. Ronda, *J. Polym. Sci. A Polym. Chem.*, 2008, **46**, 6091–6101.
41 R. Kirubakaran, P. Sharma, A. Manisekaran, J. Bijwe and L. Nebhani, *J Therm Anal Calorim*, 2020, **142**, 1233–1242.
42 B. Lochab, I. K. Varma and J. Bijwe, *J Therm Anal Calorim*, 2013, **111**, 1357–1364.
43 Z. Deliballi, B. Kiskan and Y. Yagci, *Macromolecules*, 2020, **53**, 2354–2361.
44 M. Comí, G. Lligadas, J. C. Ronda, M. Galià and V. Cádiz, *J. Polym. Sci. Part A: Polym. Chem.*, 2013, **51**, 4894–4903.
45 K. Zhang, L. Han, Y. Nie, M. L. Szigeti and H. Ishida, *RSC Adv.*, 2018, **8**, 18038–18050.
46 X. He, T. Wang, Z. Pan, A. Q. Dayo, J. Wang and W. Liu, *J Appl Polym Sci*, 2021, **138**, 50131.
47 S. Nalakathu Kolanadiyil, M. Azechi and T. Endo, *J. Polym. Sci. Part A: Polym. Chem.*, 2016, **54**, 2811–2819.
48 H. Oie, A. Sudo and T. Endo, *J. Polym. Sci. A Polym. Chem.*, 2011, **49**, 3174–3183.
49 H. Oie, A. Mori, A. Sudo and T. Endo, *J. Polym. Sci. Part A: Polym. Chem.*, 2013, **51**, 3867–3872.
50 H. Ishida and Y. Rodriguez, *J. Appl. Polym. Sci.*, 1995, **58**, 1751–1760.
51 M. A. Espinosa, V. Cádiz and M. Galià, *J. Appl. Polym. Sci.*, 2003, **90**, 470–481.
52 C. H. Lin, H. T. Lin, S. L. Chang, H. J. Hwang, Y. M. Hu, Y. R. Taso and W. C. Su, *Polymer*, 2009, **50**, 2264–2272.
53 C. Hsuan Lin, Y. R. Feng, K. H. Dai, H. C. Chang and T. Y. Juang, *J. Polym. Sci. Part A: Polym. Chem.*, 2013, **51**, 2686–2694.
54 B. Hao, R. Yang and K. Zhang, *RSC Adv.*, 2020, **10**, 25629–25638.
55 B. Hao, L. Han, Y. Liu and K. Zhang, *Polym. Chem.*, 2020, **11**, 5800–5809.
56 K. Zhang, Y. Liu, M. Han and P. Froimowicz, *Green Chem.*, 2020, **22**, 1209–1219.
57 S. Ren, X. Miao, W. Zhao, S. Zhang and W. Wang, *Materials Today Communications*, 2019, **20**, 100568.
58 Y. Zhu, P. Li, R. Lin and J. Su, *Polym. Bull.*, 2021, **78**, 4403–4417.
59 R. Lin, Y. Zhu, Y. Zhang, L. Wang and S. Yu, *European Polymer Journal*, 2018, **102**, 141–150.
60 G. Kaya, B. Kiskan and Y. Yagci, *Macromolecules*, 2018, **51**, 1688–1695.
61 2017.

62 G. M. Sheldrick, *Acta Crystallogr C Struct Chem*, 2015, **71**, 3–8.
63 G. M. Sheldrick, *Acta Crystallogr A Found Adv*, 2015, **71**, 3–8.
64 S. Vyazovkin and D. Dollimore, *J. Chem. Inf. Comput. Sci.*, 1996, **36**, 42–45.
65 S. Vyazovkin, A. K. Burnham, J. M. Criado, L. A. Pérez-Maqueda, C. Popescu and N. Sbirrazzuoli, *Thermochimica Acta*, 2011, **520**, 1–19.
66 L. Granado, R. Tavernier, G. Foyer, G. David and S. Caillol, *Thermochimica Acta*, 2018, **667**, 42–49.
67 F. W. Holly and A. C. Cope, *J. Am. Chem. Soc.*, 1944, **66**, 1875–1879.
68 H. Kanatomi and I. Murase, *BCSJ*, 1970, **43**, 226–231.
69 N. Dai, Z. Tang, M. Wang, L. Peng, Y. Wan and Y. Jiao, *Journal of Chemical Research*, 2019, **43**, 53–57.
70 S. Ohashi, K. Zhang, Q. Ran, C. R. Arza, P. Froimowicz and H. Ishida, in *Advanced and Emerging Polybenzoxazine Science and Technology*, Elsevier, 2017, pp. 1053–1082.
71 C. Wang, J. Sun, X. Liu, A. Sudo and T. Endo, *Green Chem.*, 2012, **14**, 2799.
72 A. Adjaoud, A. Trejo-Machin, L. Puchot and P. Verge, *Polym. Chem.*, 2021, **12**, 3276–3289.
73 T. Friščić, C. Mottillo and H. M. Titi, *Angewandte Chemie Intl Edit*, 2020, **59**, 1018–1029.
74 J. Ejfler, K. Krauzy-Dziedzic, S. Szafert, T. Lis and P. Sobota, *Macromolecules*, 2009, **42**, 4008–4015.
75 L. J. Farrugia, *J Appl Crystallogr*, 2012, **45**, 849–854.
76 CCDC, 12 Union Road, Cambridge CB2 1EZ, UK; Fax: +44 1223 336033; E-mail: deposit@ccdc.cam.ac.uk http://www.ccdc.cam.ac.uk/conts/retrieving.html.
77 Z.-L. Tang, Z.-H. Zhu, C.-Y. Zhang, W.-W. Chen, H.-W. Liu and K.-L. Huang, *Zeitschrift für Kristallographie - New Crystal Structures*, 2010, **225**, 147–148.
78 W. Wattanathana, Y. Hanlumyuang, S. Wannapaiboon, K. Chansaenpak, P. Pinyou, T. Nanok and P. Kanjanaboos, *Crystals*, 2021, **11**, 568.
79 L. Bonnaud, B. Chollet, L. Dumas, A. A. M. Peru, A. L. Flourat, F. Allais and P. Dubois, *Macromol. Chem. Phys.*, 2019, **220**, 1800312.
80 L. Dumas, L. Bonnaud, M. Olivier, M. Poorteman and P. Dubois, *European Polymer Journal*, 2016, **75**, 486–494.
81 L. Dumas, L. Bonnaud, M. Olivier, M. Poorteman and P. Dubois, *Green Chem.*, 2016, **18**, 4954–4960.
82 Z. Wen, L. Bonnaud, R. Mincheva, P. Dubois and J.-M. Raquez, *Materials*, 2021, **14**, 440.
83 L. Granado, R. Tavernier, G. Foyer, G. David and S. Caillol, *Chemical Engineering Journal*, 2020, **379**, 122237.
84 M. Baqar, T. Agag, H. Ishida and S. Qutubuddin, *Reactive and Functional Polymers*, 2013, **73**, 360–368.
85 A. Ručigaj, Š. Gradišar and M. Krajnc, *e-Polymers*, 2016, **16**, 199–206.
86 K. Zhang, L. Han, P. Froimowicz and H. Ishida, *Reactive and Functional Polymers*, 2018, **129**, 23–28.
87 C. Chen, Y. Cao, X. Lu, X. Li, H. Yao and Z. Xin, *Colloids and Surfaces A: Physicochemical and Engineering Aspects*, 2021, **609**, 125605.
88 X. Shen, J. Dai, Y. Liu, X. Liu and J. Zhu, *Polymer*, 2017, **122**, 258–269.
89 X. Shen, L. Cao, Y. Liu, J. Dai, X. Liu, J. Zhu and S. Du, *Macromolecules*, 2018, **51**, 4782–4799.
90 R. Sonnier, B. Otazaghine, L. Dumazert, R. Ménard, A. Viretto, L. Dumas, L. Bonnaud, P. Dubois, N. Safronava, R. Walters and R. Lyon, *Polymer*, 2017, **127**, 203–213.